Visible Light-Activated Molecular Nanomachines Kill Pancreatic Cancer Cells

Ciceron Ayala-Orozco,[‡] Dongdong Liu,[‡] Yong-Jiang Li, Lawrence B. Alemany, Robert Pal,[*] Sunil Krishnan[*] and James M. Tour[*]

[‡]These authors contributed equally.

Dr. C. Ayala-Orozco, Y.-J. Li, Prof. S. Krishnan
Department of Radiation Oncology
The University of Texas MD Anderson Cancer Center
Houston, Texas 77030, United States
E-mail: SKrishnan@mdanderson.org

Dr. D. Liu, Dr. L. B. Alemany, Prof. J. M. Tour
Department of Chemistry
Rice University
6100 Main Street, Houston, Texas 77005, United States
E-mail: tour@rice.edu

Dr. L. B. Alemany
The Shared Equipment Authority
Rice University
6100 Main Street, Houston, Texas 77005, United States

Prof. R. Pal
Department of Chemistry
Durham University
South Road, Durham DH1 3LE, UK
E-mail: robert.pal@durham.ac.uk

Prof. J. M. Tour
The Smalley-Curl Institute
The NanoCarbon Center
Department of Materials Science and NanoEngineering
Rice University
6100 Main Street, Houston, Texas 77005, United States

Keywords: molecular machines, light-activated, nanomechanical, cancer, cell death

Abstract: Recently, synthetic molecular nanomachines (MNMs) that rotate unidirectionally in response to UV light excitation have been used to produce nanomechanical action on live cells to kill them through the drilling of holes in their cell membranes. In the work here, visible light-absorbing MNMs are designed and synthesized to enable nanomechanical activation by 405 nm light, thereby using a wavelength of light that is less phototoxic than the previously employed UV wavelengths. Visible-light absorbing MNMs that kill pancreatic cancer cells upon response

to light activation are demonstrated. Evidence is presented to support the conclusion that MNMs do not kill cancer cells by the photothermal effect when used at low optical density. In addition, MNMs suppress the formation of reactive oxygen species, leaving nanomechanical action as the most plausible working mechanism for cell killing under the experimental conditions.

More methods of efficient cell killing would widen the field of available modalities for treatment of chemo-, radiation- and immuno-therapy-resistant cancers.[1],[2–5] Molecular motors and switches that change their conformation in a controllable manner in response to an external stimulus, such as light, have been demonstrated for molecular mechanical therapeutics.[6–10] Molecular mechanical therapeutics is promising because a cancer cell is unlikely to develop a defense mechanism against mechanical action. This therapeutic strategy, however, needs further development for clinical translation.

We previously showed that by using molecular machines (MNMs) with 355-365 nm light activation and motors with unidirectional rotation rates of 2-3 MHz,[11] the MNMs drilled through cell membranes causing rapid blebbing and necrosis in various types of cancer cell lines.[1] In this first generation of cell-killing MNMs, the phototoxicity of UV-light toward untargeted cells is a concern due to the potentially high level of UV-induced reactive oxygen species (ROS) and reactive nitrogen species (RNS). In order to address this secondary UV-induced damage, here we demonstrate a series of second generation, safer visible-light actuated MNMs. In our former work, we studied the treatment of single cancer cells using confocal microscopy. Here we treated colonies of *KPC* pancreatic cancer cells using MNMs, showing that cancer cells died upon 395-405 nm light emitting diode (LED) activation of the MNMs. Our results support the conclusion that MNMs work through molecular mechanical actions because the photothermal effects were minimized. In addition, we verified that MNMs do not enhance but rather quench ROS.

MNMs were designed and synthesized to absorb in the visible wavelengths of the spectrum and based upon the former work of Feringa and his group[12] (**Figure 1**, **Supporting Figure S1**, and **Scheme S1-S4**). Wavelengths of absorption are preferred outside the UV region to reduce the phototoxicity. While near infra-red (NIR) is attractive for higher penetration depth in biological tissue, the energies are too low to be useful for the MNM-induced membrane penetration. We recently used 2-photon NIR excitation of UV-activated MNM, but at the requisite high fluxes, penetration is still limited.[13] Now we have tuned the λ_{max} of absorption to ~ 405 nm for MNM **7** by introducing an amine electrodonating substituent into the conjugated core of the fast motor where the rotation rate is calculated to be in the MHz region (See Supporting Information for comprehensive discussion on the estimation of rotation rates).[12] Likewise, by introducing the methoxy electrodonating group in MNMs **5**, **6**, and **8**, the λ_{max} was tuned to 370 nm with sufficient absorption at ~ 400 nm (**Figure S1**). MNMs **1** and **3** have a λ_{max} of 401 nm but a slow rotating motor of 10^{-3} Hz. MNMs **2** and **4** have a medium speed rotating motor (10^{2} Hz) with a λ_{max} of 393 nm. All of the motors used in this study absorb 405 nm visible light (Supporting **Figure S1 and Table S1**). The side chains (hydroxyl or di(ethylene glycol)) attached to the core of the motor do not modify the λ_{max} of the photoexcitation peak that typically is in the range of 370-405 nm for the MNMs in this study.

MNMs were applied to the *LSL-Kras*$^{G12D/+}$*; LSL-Trp53*$^{R172H/+}$*; Pdx-1-Cre* cells (*KPC*), a genetically engineered mouse model of pancreatic ductal adenocarcinoma that recapitulates the biology of human pancreatic cancer.[14] Cell death on *KPC* cells is caused by visible-light activated MNMs (**Figure 2**). The cell death is quantified by the fluorescence intensity of propidium iodide (PI) intercalated into DNA or RNA in cells upon disruption of the cell membrane. PI only fluoresces upon cellular internalization and intercalation; it does not fluoresce in the cell culture medium alone. Light treatment (405 nm light for 15 min) alone does not kill the *KPC* cells during the imaging time frame of 25 min (15 min of 405 nm light activation followed by 10 min observation without light (this means the sample is maintained

in the dark). The slow rotating MNM **1** causes some minor cell death starting at 20 min (15 min of light treatment followed by 5 min observation without light). The medium rotating MNM **2** causes cell death starting at 15 min during the light treatment. In contrast, the fast rotating MNM **5** causes cell death starting ~ 5 min during the light activation. More importantly, MNM **7** caused cell death faster than MNM **5** because the λ_{max} of **7** is centered at 405 nm while the λ_{max} of **5** is centered at 371 nm. Overall, it is observed that the visible light-activated motors kill cells in the order **7** > **5** > **2** > **1**, which correlates with the respective rotation rate of 10^6 s^{-1} (**7** and **5**) > 10^2 s^{-1} (**2**) > 10^{-3} s^{-1} (**1**).

In addition to the onset time at which the cells start manifesting staining by PI, a peak in the fluorescence intensity in cells treated with **5** and **7** was observed usually at ~ 17.5 min. This peak is more evident when the individual data (not averaged) are analyzed as observed in Supporting **Figure S2-S4**. The decrease in the fluorescence intensity with time is due to the necrosis-induced blebbing and explosion-like ejection of PI-intercalated DNA or RNA into the medium which then quickly lessens in intensity due to dilution.

The cellular accumulation and clearance of MNM **7** in *KPC* cells is tracked by its fluorescence (emission spectrum in **Figure S5**). MNM **7** is imaged using filters, λ_{ex} = 405 nm and λ_{em} = 470 nm, conveniently available in most fluorescent microscopes, and applying a short time of excitation enough for imaging but not sufficient to activate the killing action of the MNM. The accumulation of **7** reaches saturation in the *KPC* cells at 1-1.5 h of incubation at 37 °C when used at 8 μM in 0.1 % DMSO (**Figure 3A** and **Figure S6**). After 1-1.5 h, the *KPC* cells start clearing **7** as suggested by the decrease of the fluorescence intensity over time (**Figure S6**). The clearance of **7** from the *KPC* cancer cells is accelerated by replacing the media as observed by the plot of the black dots in **Figure 3A**.

A 5 h clearance process removes most of **7** from the cytoplasm of *KPC* cells. This 5 h clearance involves of replacing the media 3 times at 1.5 h after the loading period, followed by

1 h incubation and replacing media 3 times, then 4 h incubation and replacing the media 3 times at 5 min before the imaging.

The 22 h clearance process removes almost all of the **7** from the cytoplasm of *KPC* cells (**Figure 3B**). Fluorescence images in **Figure 3B** support the conclusion that the fluorescence decays over time. This 22 h clearance process consists of replacing the media 3 times at 1.5 h after the loading period, followed by 1 h incubation and replacing media 3 times, then 4 h incubation and replacing the media 3 times, then 17 h incubation and replacing the media 3 times 5 min before the imaging.

To confirm that **7** is cleared over time, 405 nm light treatment is applied to the *KPC* cells at the different time points of clearance (**Figure 3C**). It is observed that as more **7** is cleared from the cell cytoplasm, the less cell death is observed when **7** and 405 nm light treatment is applied. Interestingly, there is no effect on the cell death upon light treatment when **7** was completely cleared after the 22 h clearance process was applied.

An off-the-shelf LED light is sufficient to activate the MNMs and caused cell death in *KPC* cells. The purpose of using an LED light is to demonstrate the versatility in activating the MNMs. We observed consistency in the results regardless of the activation method. Cell death was caused by MNMs upon treatment with an LED light at 395 nm for 15 min using a light power of 160 $mWcm^{-2}$ (**Figure 4**). MNMs **1**, **2** and **5** are added at 8 µM and 0.1 % DMSO in the final cell media in order to avoid unwanted cell membrane permeabilization; DMSO being required for solubility of the organic MNMs. The free MNMs are washed 3x with fresh media before the light treatment. It was observed that light treatment alone does not kill the cancer cells within the imaging time frame from 2.5-20 min after the light treatment (**Figure 4A**). For clarity in the interpretation of the results, the imaging time point in the x-axis in **Figure 4A** starts counting at zero when the 15 min light treatment is completed. However, time zero is not recorded because it takes 3 min to set up the cell culture dish in the microscope and start imaging. The MNMs alone do not kill cancer cells (**Figure 4B** and Supporting **Figure S7**).

Light-activated **2** (medium rotation rate 10^2 s^{-1}) and **5** (fast rotation rate 10^6 s^{-1}) cause cell death to the relative extents expected. In contrast, light activated slow MNM **1** initiates little cell death. The relative capacity of MNMs to kill cancer cells is **5** > **2** > **1**. This relative ability to kill cancer cells is qualitatively observed in the fluorescence images showing the internalized PI in *KPC* cells 5 min after the light treatment was completed.

To investigate photothermal effects, the temperature of the media was measured under the light treatment conditions using an LED light (395 nm light at 160 $mWcm^{-2}$ for 15 min) with or without MNM present (Supporting **Figure S8**). The results show that the light treatment alone increased the temperature of the media by only ~ 0.5 °C. The presence of 8 μM MNM **1**, the MNM with highest absorption cross section at 395 nm in this study, under the light treatment increased the temperature only 0.5 °C above the light treatment alone. This suggest that light treatments and MNMs as applied in this study cause minimal photothermal driven effects. The slow rotating MNM **1** and the medium rotating MNM **2** minimally increased the temperature of the media under the light treatment due to their larger absorption cross-section than MNM **5** (Supporting **Figure S1**). However, MNM **1** and **2** caused less cell death than MNM **5** and MNM **7** (**Figure 2** and **Figure 4**), confirming that the photothermal effect is not the dominating mechanism for cell death under the conditions in this study. To further support this conclusion, the MNM were compared at equal optical density (OD) = 0.08 under activation using LED light at 395 nm (**Figure S9**) or using light at 405 nm (**Figure S10**). If the mechanism of action were by a photothermal effect, the machines **1**, **2**, and **5** should kill the cancer cells similarly regardless of the MNM rotation rate when compared at equal OD of 0.08. However, the results at equal OD show that MNMs kill cells in the order **5** > **2** > 1, further confirming that photothermal is not the driving mechanism.

The PEGylated MNMs **3**, **4**, **6**, and **8** were applied to *KPC* cells and activated with 405 nm light or 395 nm LED light (Supporting **Figure S11-S13**). The PEGylated MNM **8** caused more cell death than MNMs **3** and **4** due to its faster rotation rate (**Figure S11**). The MNM **6**,

which is homologous in the core structure to non-PEGylated **5** and di-PEGylated **8** but different due to the single PEG arm, showed similar effect on the cell death to **5** as expected since both MNMs have the same rotation rate, therefore similar mechanical action is produced to damage cellular organelles. The MNM **4** killed the *KPC* cells faster than **3** as expected since **4** has higher rotation rate than **3**.

To confirm that ROS formation is not the mechanism of action of MNM, the ROS production during the 405 nm light treatment under the inverted fluorescent microscope was measured using CellRox^{TM} green reagent. CellRox^{TM} green dye is weakly fluorescent in its reduced form but exhibits bright green fluorescence upon oxidation by ROS and subsequent binding to DNA with absorption/emission maxima at 485/520 nm.[15] The 405 nm light treatment alone produces ROS in the *KPC* cells (**Figure 5**). The photosensitizer chlorin e6 enhances ROS production upon 405 nm light excitation.[16] In contrast, the ROS inhibitor *N*-acetyl-L-cysteine (NALC) partially quenches ROS.[17] Interestingly, the MNMs **2**, **5**, and **7** under 405 nm light treatment suppress the production of ROS relative to the light treatment alone. There has been extensive investigation of the UV-induced addition of singlet oxygen ($^1O_2$) across carbon-carbon double bonds for the photooxygenation of perylene structures.[18] This supports the observation that the twisted double bond present in the MNM structures is highly reactive to oxygen radicals, acting as a ROS quencher. MNM **5** and **7** have slightly higher ROS generation than does MNM **2** because the mechanical action by the faster MNMs likely increases ROS generation. But the bulk of ROS is quenched by the MNMs, regardless of their rotational spinning rates.

To conclude, we demonstrated that visible-light absorbing MNMs kill pancreatic cancer cells upon 405 nm light excitation. The visible-light activated MNMs work under less phototoxic conditions than our previously reported UV-light activated MNMs. We showed that MNMs were cleared from the cellular cytoplasm over time, suggesting their low toxicity as observed formerly.[1,13] Our results support the conclusion that MNMs do not kill cancer cells by

the photothermal effect under the tested conditions in this study. In addition, MNMs suppress the formation of ROS; therefore, ROS formation is not responsible for the cell death caused by MNMs. The evidence supports the conclusion that MNMs kill by mechanical action when excited by visible light. The limitation of this approach is the difficulty to treat deep seated tumors due to the poor penetration depth of blue light in biological tissue. However, this approach can be further developed for light accessible cancers such as squamous or basal cells carcinomas and other pathologic conditions in the skin.

Experimental Section

Experimental details can be found in the supporting information.

Supporting Information

Supporting Information is available from the Wiley Online Library or from the author.

Acknowledgements

Authors C. Ayala-Orozco and D. Liu contributed equally to this work. We thank Dr. Gufeng Wang for helpful discussions to optimize the LED illumination system and Dr. Pankaj K. Singh for helpful discussions on using the CellRox test. We thank Dr. Angel Marti's lab for giving us access to their fluorometer and Bo Jiang for assistance to operate the instrument. C. A.-O. was supported by the NIH Translational Cancer Nanotechnology Postdoctoral Fellowship grant T32CA196561. Dr. Pal would like to thank the Royal Society URF for funding. The work at Rice University was supported by the Discovery Institute and the Welch Foundation (C-2017-20190330).

Received: ((will be filled in by the editorial staff))
Revised: ((will be filled in by the editorial staff))
Published online: ((will be filled in by the editorial staff))

References

[1] V. García-López, F. Chen, L. G. Nilewski, G. Duret, A. Aliyan, A. B. Kolomeisky, J. T. Robinson, G. Wang, R. Pal, J. M. Tour, *Nature* **2017**, *548*, 567.

[2] P. Sharma, S. Hu-Lieskovan, J. A. Wargo, A. Ribas, *Cell* **2017**, *168*, 707.

[3] H. H. W. Chen, M. T. Kuo, *Oncotarget* **2017**, *8*, 62742.

[4] H. E. Barker, J. T. E. Paget, A. A. Khan, K. J. Harrington, *Nat. Rev. Cancer* **2015**, *15*, 409.

[5] K. M. Redmond, T. R. Wilson, P. G. Johnston, D. B. Longley, *Front. Biosci.* **2008**, *13*, 5138.

[6] A. Agarwal, H. Hess, *J. Nanotechnol. Eng. Med.* **2010**, *1*, 011005.

[7] L. Chen, M. Nakamura, T. D. Schindler, D. Parker, Z. Bryant, *Nat. Nanotechnol.* **2012**, *7*, 252.

[8] D. M. Barber, M. Schönberger, J. Burgstaller, J. Levitz, C. D. Weaver, E. Y. Isacoff, H. Baier, D. Trauner, *Chem. Sci.* **2016**, *7*, 2347.

[9] J. Broichhagen, T. Podewin, H. Meyer-Berg, Y. von Ohlen, N. R. Johnston, B. J. Jones, S. R. Bloom, G. A. Rutter, A. Hoffmann-Röder, D. J. Hodson, D. Trauner, *Angew. Chemie Int. Ed.* **2015**, *54*, 15565.

[10] M. A. Watson, S. L. Cockroft, *Chem. Soc. Rev.* **2016**, *45*, 6118.

[11] V. García-López, P.-T. Chiang, F. Chen, G. Ruan, A. A. Martí, A. B. Kolomeisky, G. Wang, J. M. Tour, *Nano Lett.* **2015**, *15*, 8229.

[12] M. M. Pollard, P. V. Wesenhagen, D. Pijper, B. L. Feringa, *Org. Biomol. Chem.* **2008**, *6*, 1605.

[13] D. Liu, V. Garcia-Lopez, R. S. Gunasekera, L. Greer Nilewski, L. B. Alemany, A. Aliyan, T. Jin, G. Wang, J. M. Tour, R. Pal, *ACS Nano* **2019**, *13*, 6813.

[14] J. W. Lee, C. A. Komar, F. Bengsch, K. Graham, G. L. Beatty, in *Curr. Protoc. Pharmacol.*, John Wiley & Sons, Inc., Hoboken, NJ, USA, **2016**, p. 14.39.1-14.39.20.

[15] H. Choi, Z. Yang, J. C. Weisshaar, *Proc. Natl. Acad. Sci.* **2015**, *112*, E303.

[16] L. Copley, P. van der Watt, K. W. Wirtz, M. I. Parker, V. D. Leaner, *Int. J. Biochem. Cell Biol.* **2008**, *40*, 227.

[17] M. Halasi, M. Wang, T. S. Chavan, V. Gaponenko, N. Hay, A. L. Gartel, *Biochem. J.* **2013**, *454*, 201.

[18] W. M. Abdou, Y. O. Elkhoshnieh, M. M. Sidky, *Tetrahedron* **1994**, *50*, 3595.

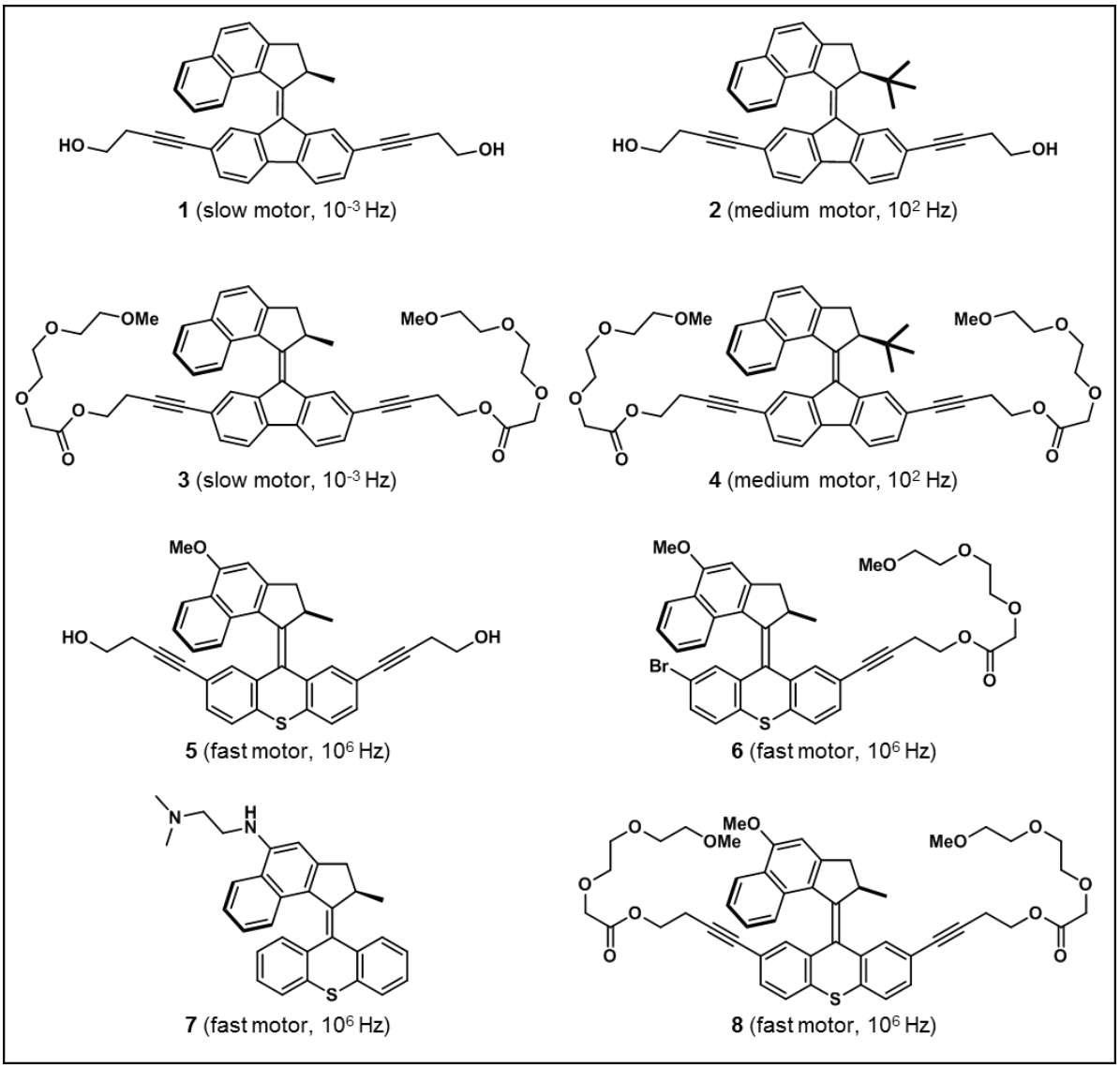

Figure 1. **Visible-light-activated MNMs**. MNMs **1** and **3** are synthesized with a slow motor in the core (10^{-3} Hz rotation rate) and varied side chains. MNMs **2** and **4** are synthesized with

motors having a medium rotation rate (10^2 Hz rotation rate) and varied side chains. MNMs **5** - **8** are synthesized with a fast motor (10^6 Hz rotation rate) and varied side chains.

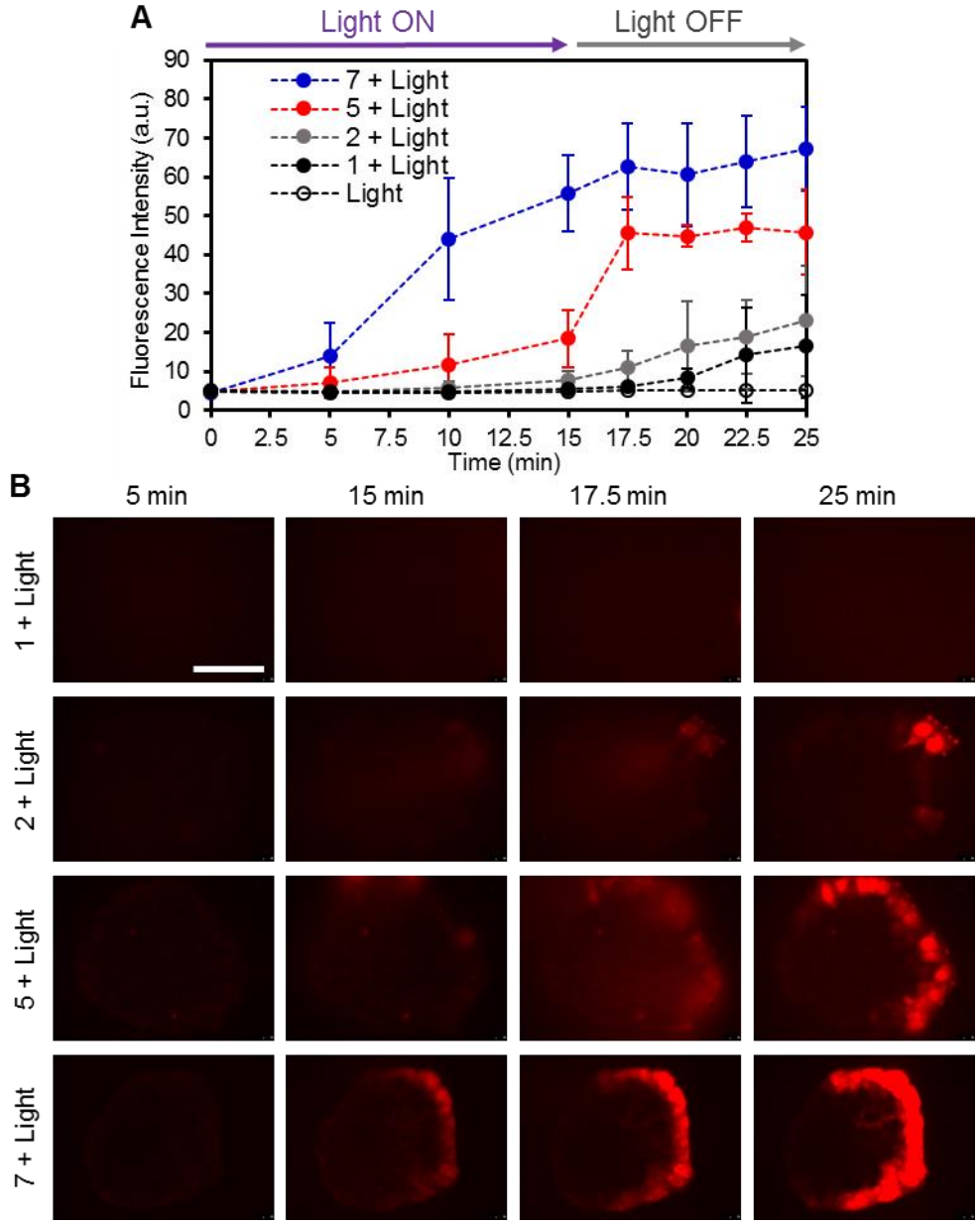

Figure 2. Cell death caused by MNMs under microscope excitation at 405 nm. **A**) Cell death is quantified by the fluorescence intensity of PI intercalation into DNA or RNA in the *KPC* cells upon cell membrane disruption. Imaging time points start when the 405 nm light is turned on. **B**) Fluorescence images of PI intercalation into DNA or RNA in *KPC* cells (for **1**, **2**, **5** fluorescence pixels are rendered in the range of 10-60 intensity to improve visualization while **7** is rendered at 0-250 pixel intensity). Samples are treated for 15 min with light using the 40x microscope objective and 405/60 nm light filter at light power of 25 mW (estimated light flux

of 500 mWcm^{-2}). MNMs concentration is 8 µM and 0.1 % DMSO and cells are incubated 1.5 h at 37 °C. Then, free MNMs in the media are washed 3x with fresh media before the light treatment. PI imaging conditions include an excitation band pass filter at 546/12 nm, dichroic mirror at 565 nm, and emission band pass filter at 600/40 nm. In all studies in this work, 0.1 % DMSO was used as a cosolvent to ensure MNM solubility. The DMSO at this concentration has no observed effect on cell behavior.[1] The bars represent standard deviation of the fluorescence intensity (~ 55 cells per field of view) across multiple experiment repetitions (n = 3). The scale bar is the same for all images = 100 µm.

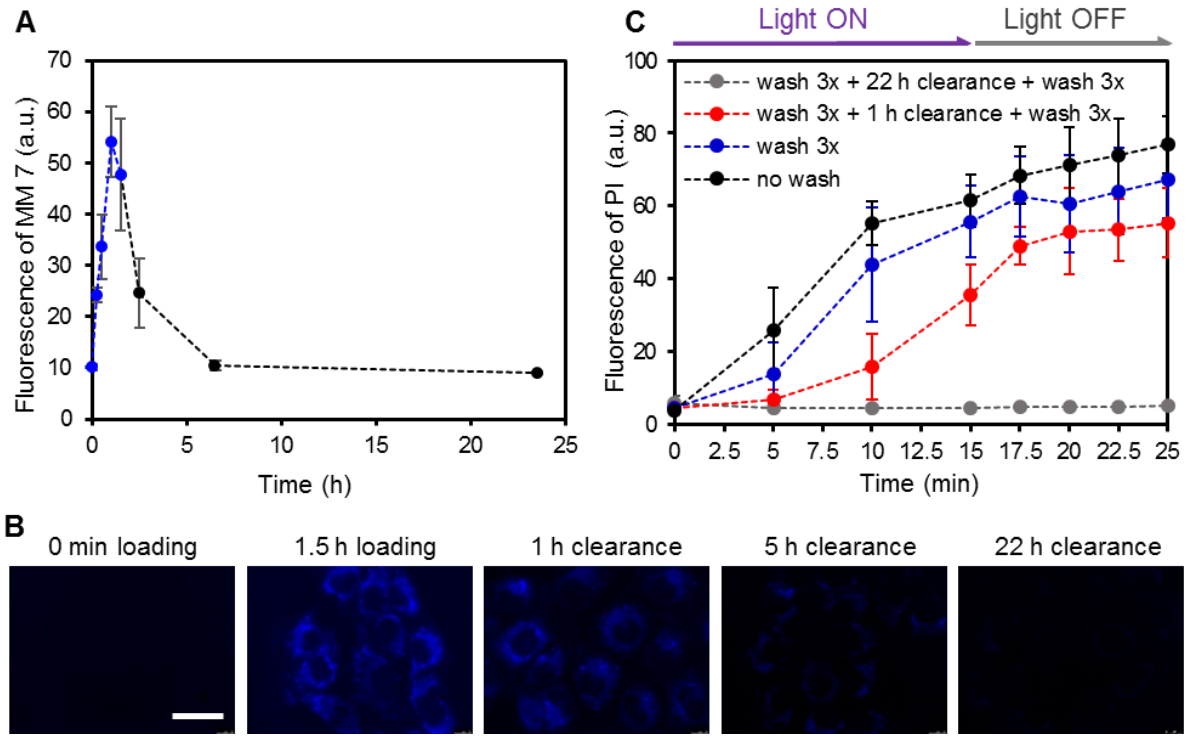

Figure 3. Loading and clearance of MNM 7 and its effect on cell death under microscope excitation at 405 nm. **A**) Fluorescence intensity of **7** in *KPC* cells. Loading (blue dots) of **7** at 8 µM in the *KPC* cells at 0.25 h, 0.5 h, 1 h and 1.5 h after incubation and washing 3x with fresh media before imaging, and clearance (black dots) upon washing 3x with fresh media at 1.5 h and continued incubation for 1 h, 5 h and 22 h. **B**) Fluorescence images of **7** loaded/cleared in the *KPC* cells. Imaging: excitation BP 405/60nm, dichromatic mirror 455 nm, and emission BP 470/40 nm. Scale bar is the same for all images = 30 µm. **C**) Cell death quantified by the internalized PI fluorescence intensity of the *KPC* pancreatic cancer cells treated with **7** at 8 µM

(1.5 h incubation at 37 °C) and 405 nm light. The PI concentration in the media was 1.5 μM in this and all other cell death experiments. The x-axis is the excitation time and post-excitation time. Light was applied after designated wash and clearance cycles were completed. Light treatments were for 15 min with the 40x microscope objective and 405/60 nm light filter at light power of 25 mW (estimated light flux of 500 $mWcm^{-2}$). PI imaging conditions used an excitation band pass filter at 546/12 nm, dichroic mirror at 565 nm, and emission band pass filter at 600/40 nm. "**No wash"**: Cells are incubated with **7** at 8 μM for 1.5 h at 37 °C and then treated with light. "**Wash 3x"**: Cells are incubated with **7** at 8 μM for 1.5 h at 37 °C, then washed 3x with fresh media, and then treated with light. "**Wash 3x + 1 h clearance + wash 3x"**: Cells are incubated with **7** at 8 μM for 1.5 h at 37 °C, then washed 3x with fresh media, then incubated 1 h, then washed 3x with media, and then treated with light. "**Wash 3x + 22 h clearance + wash 3x"**: Cells are incubated with **7** at 8 μM for 1.5 h at 37 °C, then washed 3x with fresh media, then incubated 1 h and washed 3x, then incubated 5 h and washed 3x, then incubated 17 h and washed 3x, and then treated with light. The bars represent standard deviation of the fluorescence intensity (~ 55 cells per field of view) across multiple experiment repetitions (n = 3).

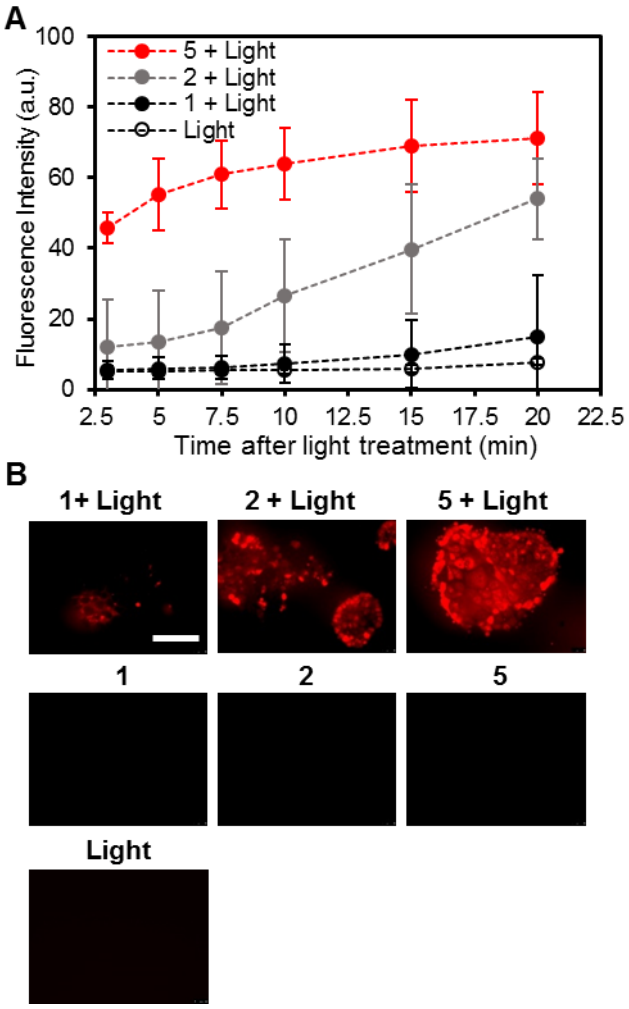

Figure 4. Cell death caused by MNM after LED 395 nm light excitation for 15 min. **A**) Cell death quantified by the fluorescence intensity of PI intercalation into DNA or RNA in the *KPC* cells. Imaging time points start 3 min after the light treatment is turned off and the fluorescence was not recorded during the 15 min of light treatment. The fluorescence intensity before the light treatment is reported in the Supporting Information Figure S7. **B**) Fluorescence images of PI intercalation into DNA or RNA in *KPC* cells at 5 min after the light treatment and control samples without light treatment. MNMs **1**, **2** and **5** are added at 8 µM and 0.1% DMSO. Then, after incubation at 37 °C for 1.5 h, unbound MNMs are partially removed by washing 3x with fresh media before the light treatment. Samples are treated for 15 min with an LED lamp at 395 nm and an average light flux of 160 $mWcm^{-2}$, placing the bottom of the LED head 1 cm above the culture dish in all the treatments. Imaging filters for PI involve excitation band pass filter at 546/12 nm, dichroic mirror at 565 nm, and emission band pass filter at 600/40 nm. The

bars represent standard deviation of the fluorescence intensity (~ 300 cells per field of view) across multiple experiment repetitions (n = 4). Scale bar is the same for all images = 150 µm.

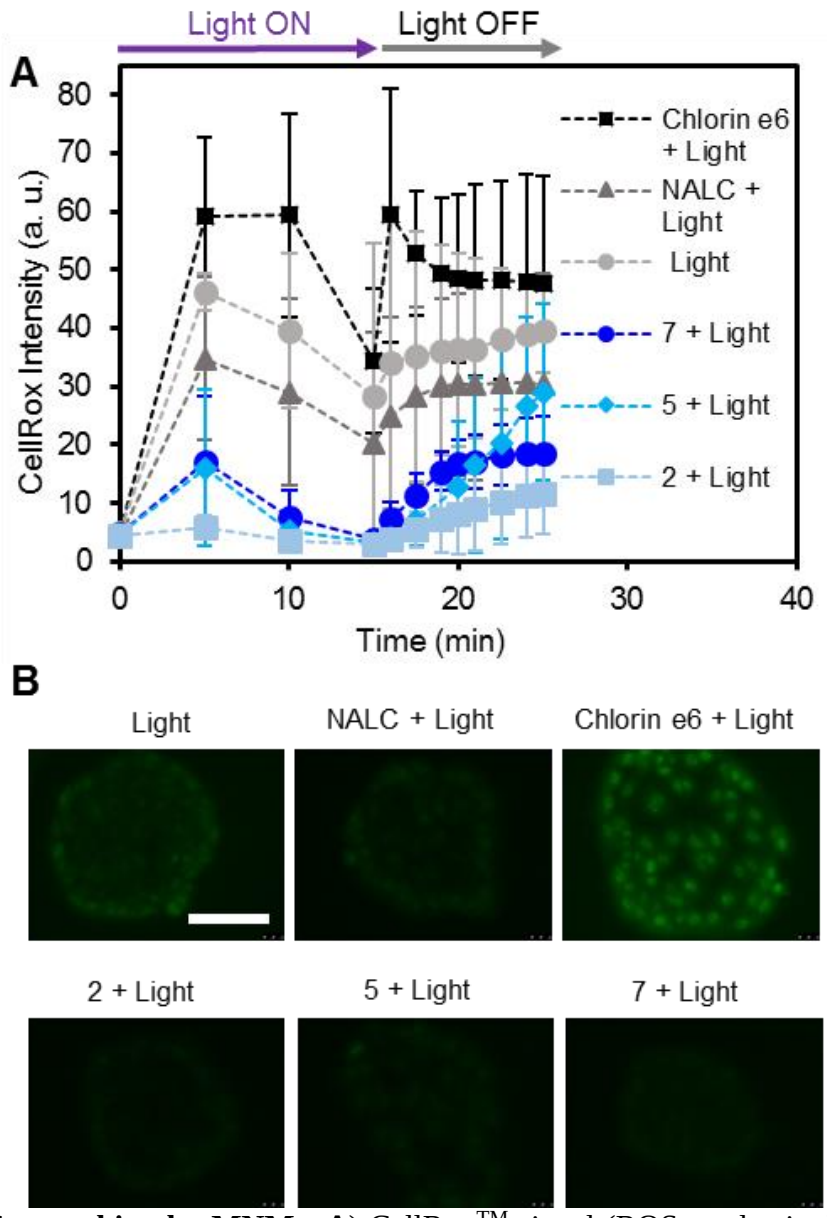

Figure 5. ROS quenching by MNMs. **A**) CellRox™ signal (ROS production) in *KPC* cells under 405 nm light excitation. Long exposure to 405 nm light causes some photobleaching of CellRox™ green reagent. **B**) Fluorescence imaging of CellRox™ (green) in *KPC* cells at 5 min of treatment with 405 nm light. Samples are illuminated for 15 min with 405 nm light under the fluorescence microscope at light power of 25 mW (estimated light flux of 500 $mWcm^{-2}$). After the light treatment, the CellRox™ signal (indicative of CellRox™ oxidation by ROS) is quantified at specific time points using excitation band pass filter at 480/40 nm, dichroic mirror

at 505 nm, and emission band pass filter at 527/30 nm. MNMs **1**, **2** and **5** are added at 8 μM, chlorine e6 and NALC were added at 8 μM, all samples contained 0.1% DMSO. The bars represent standard deviation of the fluorescence intensity (~ 55 cells per field of view) across multiple experiment repetitions (n = 3). Scale bar is the same for all images = 100 μm.

TOC abstract

Visible-light absorbing molecular nanomachines (MNMs) that kill pancreatic cancer cells upon response to light activation are demonstrated. MNMs do not kill the cancer cells by the photothermal effect when used at low optical density. In addition, MNMs suppress the formation of reactive oxygen species, leaving nanomechanical action as the most plausible working mechanism for cell killing under the experimental conditions.

Keywords

molecular machines, light-activated, nanomechanical, cancer, cell death

ToC figure